the amino acid sequence, a rather detailed characterization of the metal cluster architecture was obtained. In particular, it is worth noting that two of the Cd^{2+} ions of the four-metal cluster, i.e., Cd1 and Cd7, are bound to cysteines in relative sequence positions $i,i+2$ and $i+3$. In further work on the structural interpretation of the present experimental data (Figure 1), the conformational constraints implied by the $^{113}Cd-^{1}H$ and $^{113}Cd-^{113}Cd$ scalar couplings are being used as input for the determination of the spatial structure of MT-2 with distance geometry calculations[18] in combination with $^{1}H-^{1}H$ NOE distance constraints and the complete, sequence-specific ^{1}H NMR assignments for the polypeptide chain.

Comparison of the presently obtained results (Figure 7) with the available literature shows on the one hand that the assignment of the $^{113}Cd^{2+}$ resonances to the two clusters and the $^{113}Cd-^{113}Cd$ connectivities within the clusters are consistent with the previous proposal made by Otvos and Armitage on the basis of 1D homonuclear ^{113}Cd decoupling experiments.[7,8] On the other hand, in a hypothetical model for MT-2 proposed by the same group[17] which included sequence-specific identification of the cysteines bound to the individual Cd^{2+} ions, 18 of the proposed 28 Cd-to-cysteine connectivities are incompatible with the present experiments, including all the proposed bridging cysteines.

After this manuscript was completed, we became aware that Otvos et al.[28] and Live et al.[29] applied 2D NMR experiments related to those in Figure 2 for studies of $^{113}Cd-^{1}H$ J connectivities in MT-2 and crab metallothionein, respectively. Their experimental schemes differ from those of Figure 3 by the absence of purging procedures. There are no obvious discrepancies between the $^{113}Cd-^{1}H$ couplings identified by Otvos et al.[28] and in the present paper. The comparison of the data is limited, however, since in those studies[28] the experiments were recorded at lower frequencies and the spectra were presented in the absolute value mode with reduced spectral resolution, and no resonance assignments other than the seven Cd were given.[30]

Acknowledgments. We thank M. Sutter for the preparation of the biological material and E. H. Hunziker and R. Marani for the careful preparation of the figures and the manuscript. This research was supported by the Kommission zur Förderung der wissenschaftlichen Forschung (Project 1120), the Schweizerischer Nationalfonds (Projects 3.284-82, 3.207-82, and 2.441-82), and the Science and Engineering Research Council (UK) (Overseas postdoctoral fellowship to D. N.).

Registry No. ^{113}Cd, 14336-66-4; Cd, 7440-43-9; Cys, 52-90-4.

(28) Otvos, J. D.; Engeseth, H. R.; Wehrli, S. *J. Magn. Reson.* **1985**, *61*, 579–584.

(29) Live, D.; Armitage, I. M.; Dalgarno, D. C.; Cowburn, D. *J. Am. Chem. Soc.* **1985**, *107*, 1775–1777.

(30) Note added in proof: After this paper was submitted, we were informed that a homologous metallothionein had been studied by crystallographic methods. The crystal structure of rat liver metallothionein isoform 2 has a substantially different arrangement of cysteines than reported here. The metallothionein in the crystals contains five Cd and two Zn per mole of protein (Melis, K. A.; Carter, D. C.; Stout, C. D.; Winge, D. R. *J. Biol. Chem.* **1983**, *258*, 6255–6257. Atomic coordinates for 414 atoms (61 amino acids, 7 metals) derived from a 2.3-Å resolution electron density map were deposited June 12, 1985 with the Protein Data Bank, Brookhaven National Laboratory, Upton, NY 11973 (Furey, W. F.; Robbins, A. H.; Clancy, L. L.; Winge, D. R.; Wang, B. C.; Stout, C. D.; manuscript in preparation).

Superdegenerate Electronic Energy Levels in Extended Structures

Timothy Hughbanks

Contribution from the Department of Chemistry, The University of Chicago, Chicago, Illinois 60637. *Received February 22, 1985*

Abstract: Near singularities may occur in the electronic density of states of crystalline compounds under circumstances described in this paper. Such "superdegeneracies" are described as they result from simple Hückel treatments of various systems. Although these superdegeneracies are accidental in that they are broken when interactions ignored in the simple Hückel model are restored, large peaks in the density of states remain. The concepts presented are applied to both real and hypothetical cases. Superdegenerate bands are shown to invariably have a nonbonding character which can be fully understood only by consideration of the orbitals available for bonding in the *extended structure*. While the bands which cause superdegeneracies are flat, the Wannier functions associated with these bands cannot be well localized. The physical implications of this poor localization are discussed. In cases where superdegenerate bands are half occupied, ferromagnetic ground states appear to be favored. Analogies to molecular cases, where the importance of localizability of Hückel nonbonding molecular orbitals has already been closely examined, may point the way for the extension of this work beyond the simple one-electron treatment given here.

In chemistry and physics, particular phenomena are described by theoretical models that are meant to serve as prototypes of real systems. The features of the models that are associated with these phenomena are often implicitly assumed to be necessary conditions for the occurrence of the phenomena in question. Such is the case in the explanation of narrow electronic energy bands and the concomitant peaks associated with these bands in crystalline solids. Narrow bands naturally arise when overlaps between atomic orbitals centered on neighboring atoms throughout a crystal are small. In the regime of small interatomic or intermolecular interaction, crystalline charge densities will differ little from those of the constituent atoms, molecules, or ions. The outgrowth of these observations is the assumption that narrow energy bands are to be found *only* when a system is characterized by at least one set of weakly interacting atomic or molecular orbitals. Simple physical prototypes in solid-state theory often ignore the kinds of subleties that specific structures may possess. This paper presents a discussion of cases in which flat bands are a consequence of the pseudo-symmetry of the extended structure of a solid *as a whole*. The underlying reasons for the occurrence of these highly degenerate bands are revealed by examining systems in the light of the simple Hückel model and its ability to uncover features that have a topological origin. The presentation is meant to be suggestive, and it is hoped that it will stimulate investigation into the ways in which particular extended structures show unusual properties because of these superdegenerate bands.

0002-7863/85/1507-6851$01.50/0

A Prototypical Example

In conventional LCAO treatments of crystalline solids[1] (i.e., tight-binding methods), one begins with a symmetry-adapted basis set of orbitals $\{\phi_\mu(\mathbf{k})\}$ that are Bloch sums of AO's, $\{\phi_\mu(\mathbf{r}-\mathbf{R})\}$, of the N unit cells of the crystal:

$$\phi_\mu(\mathbf{k}) = \frac{1}{N^{1/2}}\sum_{\mathbf{R}} e^{i\mathbf{k}\cdot\mathbf{R}}\phi_\mu(\mathbf{r}-\mathbf{R}) \tag{1}$$

The sum over $\mathbf{R}$ extends over the unit cells of the crystal; the function $\phi_\mu(\mathbf{r}-\mathbf{R})$ is the μth AO of a unit cell associated with the lattice site specified by $\mathbf{R}$. The factor $e^{i\mathbf{k}\cdot\mathbf{R}}$ is the phase change in the orbitals $\{\phi_\mu(\mathbf{k})\}$ on moving from a given reference cell (at the origin) to a cell at the site specified by $\mathbf{R}$. The set $\{\phi_\mu(\mathbf{k})\}$ is symmetry adapted in that the *translational* symmetry has been fully exploited in employing this basis. Thus, the full crystal orbital problem is divided into separate problems for each wavevector $\mathbf{k}$, each problem having the dimension of the number of AO's per unit cell. The periodicity of $e^{i\mathbf{k}\cdot\mathbf{R}}$ with respect to $\mathbf{k}$ allows one to restrict $\mathbf{k}$ to the first Brillouin zone in $\mathbf{k}$ space. Further details are available in standard texts.[1b,c]

Crystal orbitals obtained by solution of the secular equation using the Bloch basis functions of eq 1 are expressed as a linear combination of Bloch functions for each $\mathbf{k}$:

$$\psi_n(\mathbf{k}) = \sum_\mu c_{\mu n}(\mathbf{k})\phi_\mu(\mathbf{k}) \tag{2}$$

where n is the so called "band index" and runs from 1 to the number of atomic orbitals in the unit cell, as does μ. At this point it should be noted that the set of Bloch basis functions, $\{\phi_\mu(\mathbf{k})\}$, need not be built from AO's, but may consist of MO's or fragment MO's or any other convenient (but equivalent) basis. In particular, we may choose to transform to a basis set that is *explicitly* $\mathbf{k}$ dependent. We may, for example, wish to make a change in basis involving $\phi_1(\mathbf{k})$ and $\phi_2(\mathbf{k})$:

$$\phi_1'(\mathbf{k}) = \frac{1}{\sqrt{1+|\lambda_\mathbf{k}|^2}}[\phi_1(\mathbf{k}) + \lambda_\mathbf{k}\phi_2(\mathbf{k})] \tag{3a}$$

$$\phi_2'(\mathbf{k}) = \frac{1}{\sqrt{1+|\lambda_\mathbf{k}|^2}}[-\lambda_\mathbf{k}^*\phi_1(\mathbf{k}) + \phi_2(\mathbf{k})] \tag{3b}$$

where $\lambda_\mathbf{k}$ is a complex number that varies with $\mathbf{k}$. Naturally, the coefficients in eq 2 are transformed in the new basis as well since $\psi_n(\mathbf{k})$ will not depend on the basis:

$$c_1'(\mathbf{k}) = \frac{1}{\sqrt{1+|\lambda_\mathbf{k}|^2}}[c_1(\mathbf{k}) + \lambda_\mathbf{k}^* c_2(\mathbf{k})] \tag{4a}$$

$$c_2'(\mathbf{k}) = \frac{1}{\sqrt{1+|\lambda_\mathbf{k}|^2}}[-\lambda_\mathbf{k} c_1(\mathbf{k}) + c_2(\mathbf{k})] \tag{4b}$$

Inasmuch as the coefficients $c_1(\mathbf{k})$ and $c_2(\mathbf{k})$ already contain the $\mathbf{k}$ dependence of the contribution of $\phi_1(\mathbf{k})$ and $\phi_2(\mathbf{k})$ to $\psi_n(\mathbf{k})$, the transformation accomplishes nothing in a formal sense. Nevertheless, as we shall see in the examples to follow, it is more convenient to consider transformations such as that in eq 3 than dealing with the problem of finding the coefficients $\{c_{\mu n}(\mathbf{k})\}$ in eq 2. More important, there will be a conceptual advantage to performing the transformation of eq 3 as merely another step in preparing a symmetry-adapted basis whether or not any "calculation" is performed.

The area of application of polyatomic molecular orbital theory with which chemists are probably most familiar is that of aromatic hydrocarbons. Specifically, the use of simple Hückel theory to produce a qualitative spectrum of energy levels for planar aromatics has a time-honored place in the training of chemists. Therefore, to first demonstrate the phenomenon of superdegeneracy in an extended system, we will consider a hypothetical problem in an extended two-dimensional net. Consider the net, **1**, consisting of an infinite collection of fused three- and nine-membered rings. One may think of this as an unlikely alternative to graphite for which we wish to know the π energy levels. The simplest way to proceed in this problem is to divide the unit cell into fragments of which it is composed. Therefore, we will proceed by considering the interaction of the π molecular orbitals of the triangle (of a_1'' and e'' symmetry) with the pπ orbital (called ϕ) of the single trigonal atom that links these triangles together (see **2**). We will refer to the Bloch basis orbitals corresponding to

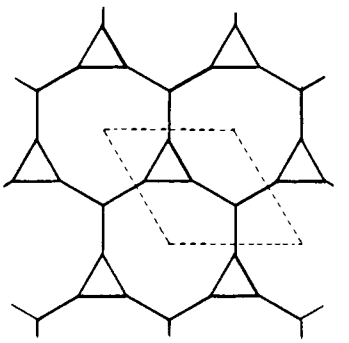

1

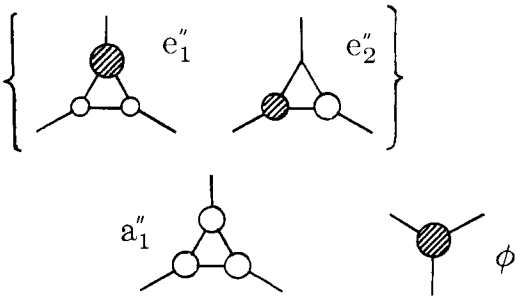

2

these fragment orbitals as $a_1''(\mathbf{k})$, $\{e_1''(\mathbf{k}), e_2''(\mathbf{k})\}$, and $\phi(\mathbf{k})$. These are defined as in eq 1.

Instead of proceeding to a solution of the crystal orbital problem, let us note that there is an illuminating transformation that can be performed that simplifies matters. Let us define a $\mathbf{k}$-dependent linear combination of the two degenerate $e''(\mathbf{k})$ functions, to be called $\chi(\mathbf{k})$, subject to the condition that $\chi(\mathbf{k})$ does not interact with the orbitals on the linking atoms ($\phi(\mathbf{k})$) for *any* $\mathbf{k}$:

$$\chi(\mathbf{k}) = \frac{1}{\sqrt{1+|\lambda_\mathbf{k}|^2}}[e_1''(\mathbf{k}) + \lambda_\mathbf{k} e_2''(\mathbf{k})] \tag{5a}$$

such that

$$\langle\phi(\mathbf{k})|H_{\text{eff}}|\chi(\mathbf{k})\rangle = 0 \tag{5b}$$

where $\lambda_\mathbf{k}$ is determined by condition 5b. H_{eff} in (5b) is the effective Hückel Hamiltonian. These two equations lead to an expression for $\lambda_\mathbf{k}$:

$$-\lambda_\mathbf{k} = \frac{\langle\phi(\mathbf{k})|H_{\text{eff}}|e_1''(\mathbf{k})\rangle}{\langle\phi(\mathbf{k})|H_{\text{eff}}|e_2''(\mathbf{k})\rangle} \tag{6}$$

For any $\mathbf{k}$, this expression may be evaluated to yield $\chi(\mathbf{k})$ (unless the denominator is zero; then $\chi(\mathbf{k}) = e_2''(\mathbf{k})$). We can infer that *for every* $\mathbf{k}$ there will be one orbital with the energy of the e'' ring orbitals because $\chi(\mathbf{k})$ is completely decoupled from the linking trigonal atoms. For a crystal with N ($\sim 10^{23}$) cells there will be a N-fold degeneracy at $E = -\beta$, the energy of a e'' orbital for a single triangle in the simple Hückel model. This is graphically shown in Figure 1 in which the density of states for this system

(1) The "renaissance" of the tight-binding method is surveyed in (a) "Solid State Physics. Advances in Research and Applications," Ehrenreich, H., Seitz, F., Turnbull, D., Eds.; Academic Press: New York, 1980; Vol. 35. See also: (b) Harrison, W. A. "Solid State Theory"; Dover: New York, 1980. (c) Ashcroft, N. W.; Mermin, N. D. "Solid State Physics"; Holt, Rinehart and Winston, New York, 1976.

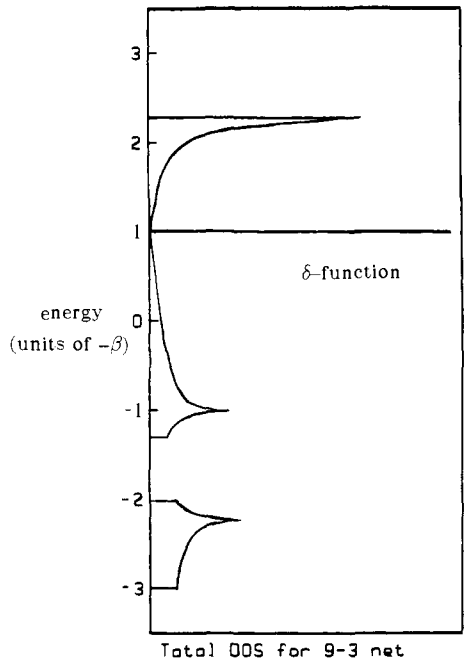

Figure 1. Density of states for the Hückel problem associated with the 9–3 net. The δ-function at $-\beta$ is the superdegenerate band. All wave functions associated with the superdegenerate band are localized on the three-membered rings.

is shown. Since this system has not been introduced for its intrinsic interest, we will not dwell on other details of the DOS.[2]

To strip away some of the formality of the above discussion, let us examine how this "accidental" degeneracy occurs for this system. Because of the translational symmetry of our hypothetical net, we are able to specify for each crystal orbital the relative phase it must display on moving from cell to cell. Since there is but one trigonal linking atom per cell, the contribution that this atom's $p\pi$ orbital makes to any given crystal orbital (i.e., an orbital with specified wavevector **k**) is *fixed everywhere* in the crystal once the phase at one site is chosen. Thus, the "environment" of the triangles is determined once and for all for each **k** (see **3**). Since

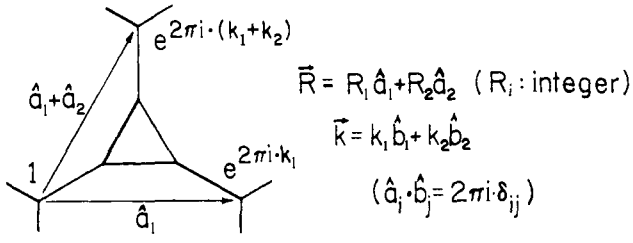

3

only nearest-neighbor interactions are retained in a simple Hückel approach and because the two e″ orbitals are degenerate, a linear combination of the two components of e″ that is orthogonal to the linking atom orbitals will be unperturbed from its "free molecule" energy of $-\beta$. A linear combination of these *two* degenerate basis functions can always be found that satisfies the *single* constraint that it be orthogonal to the linking atom orbitals. Qualitatively, the superdegenerate band of ring e″ levels occurs because there are not enough orbitals on the intervening trigonal atoms to "satisfy" them. This is a general feature of superdegenerate orbitals; they are nonbonding. In this instance, they are nonbonding with respect to linkages between the triangles and the linking trigonal atoms. Note that every $\chi(\mathbf{k})$ (for all **k**) is orthogonal to the set of linking atom orbitals, $\{\phi(\mathbf{k})\}$. They are therefore orthogonal to each localized $\phi(\mathbf{r}-\mathbf{R})$ because these localized functions were, after all, used to construct the set $\{\phi(\mathbf{k})\}$ in the prescription of eq 1. This property helps one to visualize the restrictions on the localization of states involving superdegenerate band orbitals as we will see below.

(2) A discussion of the 9–3 net and other two-dimensional nets can be found in: Burdett, J. K.; Lee, S. *J. Am. Chem. Soc.* **1985**, *107*, 3050.

π Levels of ReO_3

As a more realistic example in which superdegeneracies can occur, let us consider the π system of ReO_3. This compound has the structure depicted in **4**, in which Re atoms form a simple cubic

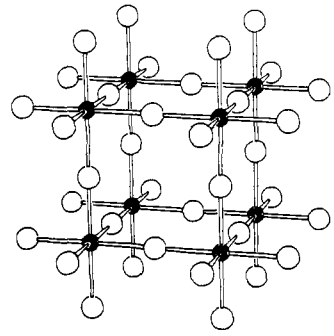

4

array and are bridged by oxygens. Each Re is surrounded by an octahedron of oxygens and each oxygen is linear. Besides being of interest in its own right, ReO_3 is closely related, structurally and electronically, to the well-known perovskites that have the formula ABO_3. In these compounds the cubic "boxes" evident in **4** are stuffed with any of a number of large cations while Re is replaceable with a wide variety of early transition metals and main group metals. The following description of the Re–O π bonding will extend with varying degrees of applicability to the perovskites as well. Neglecting any orbital interactions other than those between nearest neighbor Re and O, the atomic orbitals on each center can be cleanly divided into σ- and π-type orbitals.

Adopting the natural Cartesian coordinate system at the Re sites, the s, $\{p_x,p_y,p_z\}$, and $\{d_{z^2},d_{x^2-y^2}\}$ orbitals on this atom are classified as having σ character while the $\{d_{xy},d_{xz},d_{yz}\}$ orbitals participate in π bonding only. The linear oxygens each have s and $p\sigma$ orbitals as well as two $p\pi$ orbitals. Although the Re p orbitals and the O $p\pi$ orbitals are not orthogonal, we may anticipate that the σ interactions will be much more important, and so we can reasonably neglect any Re p contributions to π bonding. Therefore, the π bonding problem in this compound reduces to a consideration of the Re–O $d\pi$–$p\pi$ interactions. Further simplification of the π-electron problem for ReO_3 is realized by separating the interactions in the *xy*, *xz*, and *yz* planes. The retention of only nearest-neighbor interactions makes this separation exact, as can be seen by inspection of **5**, where orbitals that

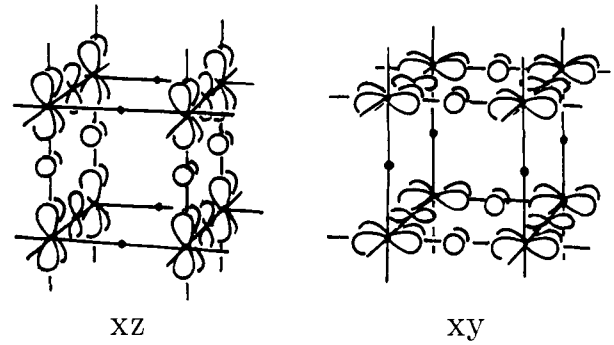

5

lie in the *xy* and *xz* planes are shown. Since each of the $d\pi$ orbitals may only participate in δ interactions with any center that lies on a line normal to the plane in which they extend, the $p\pi$ orbitals of the linking oxygens cannot couple these systems together. So we need only solve a two-dimensional band problem in which there are three basis orbitals per unit cell; see **6**.

The ReO_3 π problem is now reduced to its essentials. Since our simple Hückel model neglects any interactions between next-nearest-neighbor oxygens, we are free to construct a **k**-de-

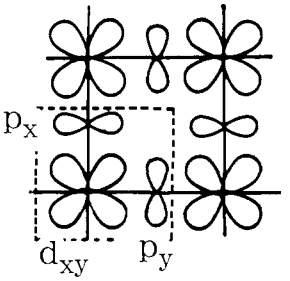

6

pendent linear combination of the p-orbital Bloch functions, just as we did for the e″ orbitals in our previous example. That is, we define a function $\chi(\mathbf{k})$ in a fashion analogous to before:

$$\chi(\mathbf{k}) = \frac{1}{\sqrt{1 + |\lambda_k|^2}}[p_x(\mathbf{k}) + \lambda_k p_y(\mathbf{k})] \quad (7a)$$

such that

$$\langle d_{xy}(\mathbf{k})|H_{\text{eff}}|\chi(\mathbf{k})\rangle = 0 \quad (7b)$$

where λ_k is determined by condition 7b. Just as before, these two equations lead to an expression for λ_k:

$$-\lambda_k = \frac{\langle d_{xy}(\mathbf{k})|H_{\text{eff}}|p_x(\mathbf{k})\rangle}{\langle d_{xy}(\mathbf{k})|H_{\text{eff}}|p_y(\mathbf{k})\rangle} \quad (8)$$

Here, because $\chi(\mathbf{k})$ does not interact with $d_{xy}(\mathbf{k})$, there should appear a dispersionless band at the energy of a free oxygen p orbital. All of this is, of course, fully analogous to our prototypical π-electron Hückel problem. The orthonormal combination of $p_x(\mathbf{k})$ and $p_y(\mathbf{k})$ *will* interact with $d_{xy}(\mathbf{k})$, and a 2 × 2 secular equation can be set up involving these functions. The details are explicitly worked through in Appendix I; here we present the π DOS which results in Figure 2.

A comparison of this model with more elaborate treatments is favorable in that the essential *form* of the π density of states for ReO_3 is captured in our simple model. Figure 3 shows the density of states reported by Mattheiss[3] for this system. The δ-function associated with the flat superdegenerate band is, of course, broadened in this calculation. This broadening is due mostly to O–O interactions that are ignored in the nearest-neighbor model. However, the nature of the crystal orbitals associated with this band are well described by the model; in contrast with the broader lower lying Re(d)–O(p) π bonding band, there is no Re(d) contribution in the superdegenerate band. This feature persists in extended Hückel calculations on this system. The steepness in the rise of the band edges reported by Mattheiss is characteristic of the two-dimensional nature of the bands and is shown in the model density of states. More discussion of the chemical inferences one can draw from our results will be presented elsewhere.[4]

Nonbonding Orbitals

The systems discussed above exhibit superdegeneracies which are fairly "unadulterated". We can identify the structural features that underlie the existence of superdegenerate bands using a simple model, and when we move to a better description of the electronic structure the general features of these bands suffer little alteration. At the cost of some of this exactitude, extension of these ideas can be achieved and applications to more interesting systems can proceed. From the chemist's point of view, the most interesting systems are those in which the occurrence of superdegeneracies fundamentally alters our overall bonding picture and/or when superdegenerate bands are among the frontier orbitals and may even be partially occupied.

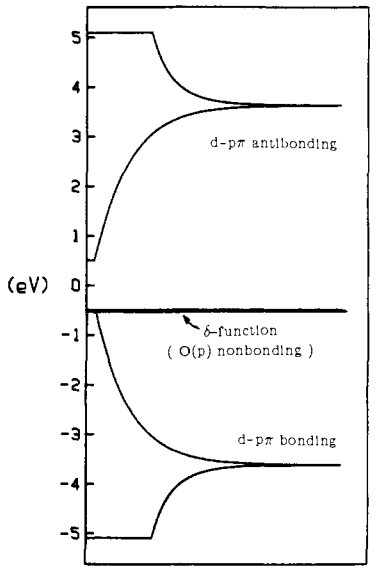

Figure 2. The density of states for a simple Hückel treatment of the π orbitals of ReO_3 is shown. The lower band has Re–O π-bonding character, while the upper has π-antibonding character. The δ-function is the O(p) superdegenerate band.

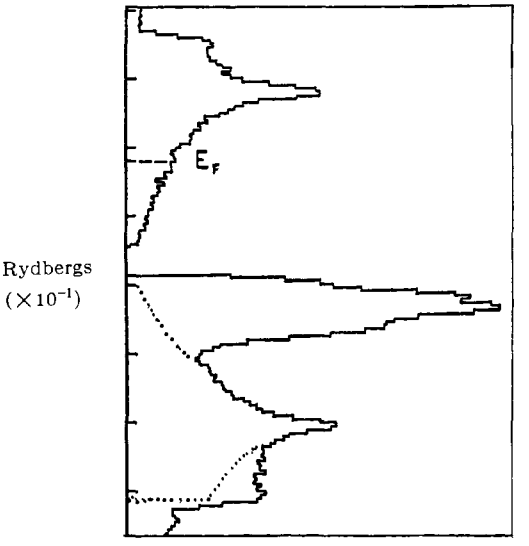

Figure 3. The density of states for ReO_3 calculated by Mattheiss using a LCAO fitting to augmented plane wave results. The dotted line shows the oxide pπ bonding band as it would appear if not obscured by the nonbonding peak at top and a p σ band at bottom (adapted from ref 3).

The structures of a series of compounds with the general formula A_2MX_2 (A = Na, K, Rb; M = Pd, Pt; X = P, As) are known in which $^1_\infty[MX_2^{2-}]$ chains such as those depicted in **7** are found.[5]

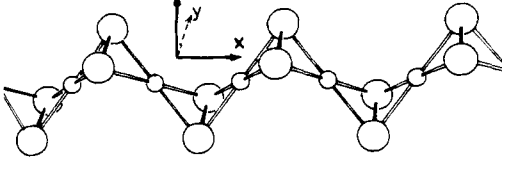

7

These chains may be described as a zig-zag fusion of $Pt(As_2)_2$ bow-ties in which As_2 units are shared between adjacent metals. The M–M distances are rather long (greater than 3.1 Å) and may be regarded as having negligible influence on the qualitative bonding picture for this system. Although these compounds have

(3) (a) Mattheiss, L. F. *Phys. Rev.* **1969**, *181*, 987; *Phys. Rev. B: Condens. Matter* **1972**, *6*, 4718. (b) Theoretical and experimental results appear in: Wertheim, G. K.; Mattheiss, L. F.; Campagna, M.; Pearsall, T. P. *Phys. Rev. Lett.* **1974**, *32*, 997.

(4) (a) Wheeler, R. A.; Whangbo, M.-H.; Hughbanks, T.; Hoffmann, R.; Burdett, J. K.; Albright, T. A., submitted for publication. (b) Burdett, J. K.; Hughbanks, T., in preparation.

(5) (a) Schuster, H.-U.; Rõsza, S. *Z. Naturforsch., Teil B* **1979**, *34*, 1167. (b) Rõsza, S.; Schuster, H.-U. *Ibid.* **1981**, *36*, 1666.

been included in a useful theoretical study that explored structural and electronic interrelationships among a variety of compounds,[6] they will be reexamined here as an illustration of how the viewpoint taken in this work serves to clarify some essential aspects of bonding.

In describing these systems, it is difficult to decide what formal electron count is appropriate to assign the As_2 dimers and the Pt atoms. If we think of As_2 as isoelectronic with disulfide (S_2^{2-}), then we have chains which we may formulate as $^1_\infty[Pt^{2+}(As_2)^{4-}]^{2-}$. This is consistent with our knowledge of Pt(II) stereochemistry if we consider the metals to possess a square-planar coordination environment and should therefore be d^8, 16 e centers. As helpful as this kind of thinking can often be, in this case it probably misleads more than it explains.

The orbitals of the As_2 dimers which are principally utilized in bonding to the Pt atoms are the diatomic's π and π^* orbitals because they extend into the interatomic region between these fragments and therefore overlap best with the metal-based orbitals. The role of the As_2 π levels may be unambiguously defined as donating to the metal. This is simply because the π levels lie deep in energy with respect to the valence orbitals on the metal (d, s, and p). How we are to think about the As_2 π^* levels is a different matter. Because these orbitals are antibonding within the As_2 dimer, they are pushed well above the energy of an As p orbital. Since As is not very electronegative compared with Pt, the result is that the As_2 π^* orbitals lie well above the metal d levels. Still, because the π interaction in As_2 is weaker than that found for HCCH, the As_2 π^* levels are still well below the metal p levels. With these considerations in mind, let us proceed to analyze the bands in $^1_\infty[Pt(As_2)^{2-}]$ chains which are *antisymmetric with respect to the xz plane* defined in **7**. To begin with, we will consider only the As_2 π^* levels and metal d_{xy} and d_{xz} orbitals in our bonding picture.

To get to the essentials of the Pt d–As_2 π^* interaction, even further simplification is possible. Considering each metal's local coordination by the adjacent As_2 ligands, all d–π^* overlaps can be decomposed into a combination of the fundamental in-plane or out-of-plane overlaps illustrated in **8**. The out-of-plane overlap

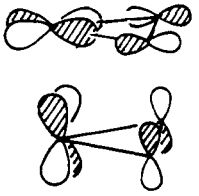

$$<d_{\text{in-plane}} \mid \pi^*> = .149$$

$$<d_{\text{out-of-plane}} \mid \pi^*> = .048$$

8

is smaller by a factor of 0.32 than the in-plane overlap, as calculated using the EH parameters given in Appendix II. This is because the relatively acute As–Pt–As angle (57°) reduces the d–p π overlap involved in the out-of-plane interaction (**8**) while the in-plane overlap has a fairly large d–p σ component. Second-order perturbation theory gives us an estimate of the relative importance of these two overlaps via an expression for the energy shift resulting from the interaction of two levels:[7]

$$\Delta E = |H_{ij}|^2/(E_i^{(0)} - E_j^{(0)}) \qquad (9)$$

Assuming, as in the Wolfsberg–Helmholz approximation, H_{ij} is proportional to S_{ij}, the As_2 π^* levels are shifted $1/(0.32)^2$ ($\simeq 10$) times as much by in-plane interactions as out-of-plane interactions. Therefore, we may safely neglect the out-of-plane d orbitals insofar as they perturb the As_2 π^* levels.

With the preliminary machinations out of the way, we are once again confronted with the ingredients for the formation of a superdegenerate band. We have *two* As_2 π^* orbitals per unit cell and only one Pt d orbital which can effectively interact with them. Just as for the previous examples, a nonbonding As_2 π^* band will emerge in the DOS for this system. On the other hand, one combination of the π^* levels *will* interact with the in-plane d orbitals and will be destabilized. The results are schematically given in **9**; the As_2 π^* levels are split to form two bands. This

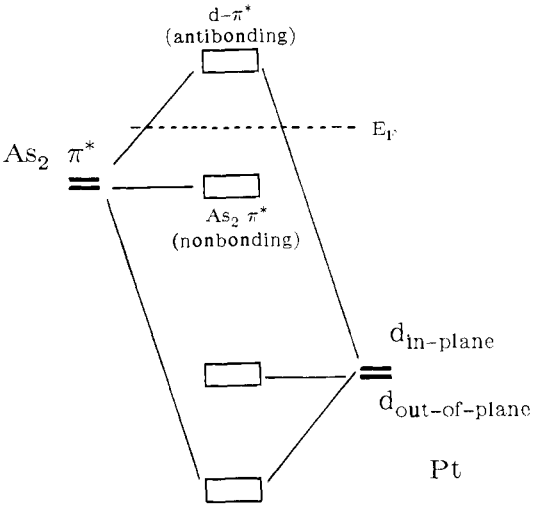

9

splitting is important because the Fermi level lies between these two bands and the formal π-electron configuration for the As_2 dimer is $(\pi_u)^4(\pi_g^*)^2$. Thus we have a sound basis for formulating this chain as $^1_\infty[Pt^0(As_2^{2-})]$. In contrast to a ligand field viewpoint, the Pt d levels do not make the predominant contribution to either the valence or conduction bands for this system. The band gap depends on the splitting of the As_2 π^* levels that we have focused on here. Detailed calculations[6] bear this out except for some uncertainty in the valence band where some symmetric bands cross the nonbonding π^* bands.

There are some caveats to bear in mind for this system. The Pt p_y orbital does have a modest influence on the energy of the nonbonding As_2 π^* band. Since the p_y orbital lies high in energy the As_2 π^* band is moderately *stabilized* by interaction with the Pt p_y orbital (recall, although the nonbonding π^* orbitals are orthogonal to the in-plane Pt d orbitals, they are not orthogonal to the p_y orbital). Thus, if the Pt p_y orbital is included in the picture, the As_2 π^* orbitals are seen to have two roles: as *acceptors* toward the Pt d orbitals and as *donors* toward the Pt p orbitals. The recognition of the As_2 nonbonding π^* band (toward the Pt d orbitals) makes this dual role easily understood.

An intriguing extension of the ability of As_2 π^* orbitals to serve as key nonbonding frontier orbitals may be envisioned for hypothetical two-dimensional systems with the stoichiometric formula $A_2[M_3(X_2)_2]$ (A = Cs, Rb; M = Pt, Pd; X = As, P). In such a compound As_2 dimers might form a hexagonal honeycomb structure as depicted in **10**; this structure is identical with the

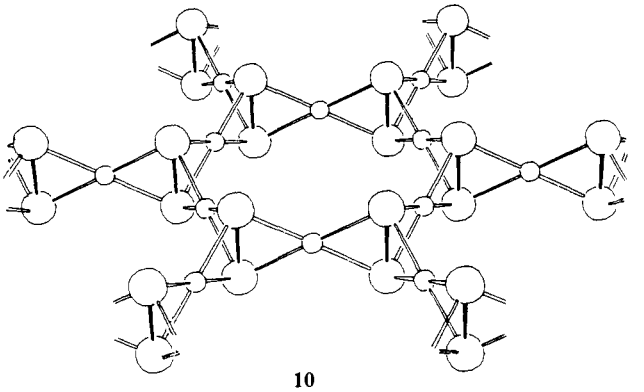

10

known structure of $A_2M_3S_4$ compounds[8] except that in the latter

(6) Underwood, D. J.; Nowak, M.; Hoffmann, R. *J. Am. Chem. Soc.* **1984**, *106*, 2837.

(7) Hoffmann, R. *Acc. Chem. Res.* **1971**, *4*, 1.

(8) (a) Huster, J.; Bronger, W. *J. Solid State Chem.* **1974**, *11*, 254. (b) Günther, O.; Bronger, W. *J. Less Common Met.* **1973**, *31*, 255. See also the cyclic hexamer $[Ni(SC_2H_5)_2]_6$ reported in: (c) Woodward, P.; Dahl, L. F.; Abel, E. W.; Crosse, B. C. *J. Am. Chem. Soc.* **1965**, *87*, 5251.

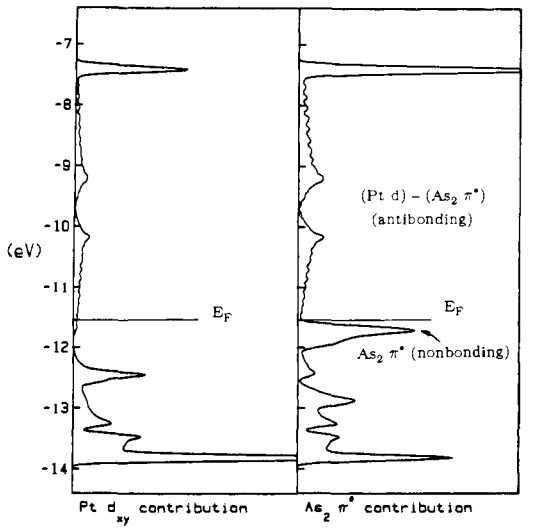

Figure 4. The As_2 π^* and Pt in-plane contributions to the density of states for a two-dimensional $Pt_3(As_2)_2^{2-}$ layer are shown. The "in-plane" d orbital is defined relative to the adjacent As_2 dimers as depicted in **8**. Note the position of the Fermi level and the superdegenerate As_2 π^* band.

no S–S bonds are found. The As_2 coordination suggested in this structure has precedent in $[M(CO)_5]_3(X_2)$ molecules (M = W or Mo; X = As, Sb, or Bi); see **11**. Such a system may also be

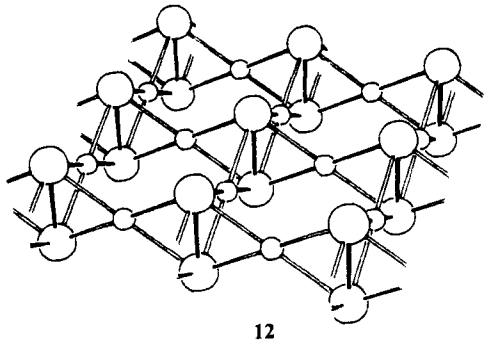

12

viewed as a hexagonal analogue to the tetragonal structure recently reported[10] for $BaPd_2X_2$ (X = P, As) in which X_2 dimers are found in layers as illustrated in **12**. The Pd centers have the same

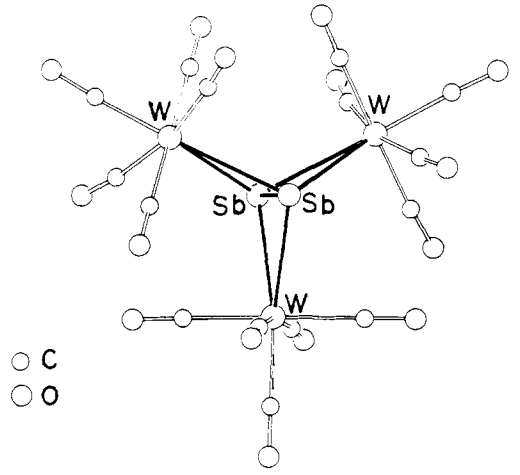

11

bow-tie coordination found in K_2PtAs_2 and in the proposed hexagonal structure **10**. The $^2_\infty[M_3(X_2)_2^{2-}]$ net contains two X_2 dimers and therefore *four* π^* orbitals per unit cell. By reasoning exactly parallel to that outlined in treating the $^1_\infty[Pt(As_2)^{2-}]$ chains, we know there are *three* metal d orbitals which may effectively interact with them. Therefore, one As_2 π^* band will be left nonbonding and will lie relatively low in energy. An extended Hückel calculation on this system underscores this conclusion. Figure 4 shows the As_2 π^* and Pt in-plane d contributions to the density of states for a $^2_\infty[Pt_3(As_2)_2^{2-}]$ system. There is considerable mixing of these levels throughout the energy range *except* that the peak present just below the Fermi level in the As_2 π^* contribution has no counterpart in the Pt d part. Just as in the $^1_\infty[Pt(As_2)^{2-}]$ chains, an As_2 nonbonding π^* band is the valence band.[11] Because of the detailed nature of the Pt d–As_2 π^* antibonding bands, they extend down to "touch" the nonbonding band and this material should be metallic.

The above cases are ones in which the requirements for superdegenerate bands are loosened somewhat with the dividend of some generalization. We can infer the existence of nonbonding bands in an extended system merely by inspection of the *extended* structure and careful consideration of the orbitals available for bonding. The most ambitious goal is the realization of a system in which the superdegenerate bands are quite narrow and only partially occupied. One hypothetical but plausible candidate may be constructed (on paper) from the 9–3 net by an isolobal replacement.[12] The crucial ingredient of the 9–3 net that led to a superdegenerate band is the set of e″ orbitals of the three-membered ring. If we replace the three-membered ring with a linear ML_2 group, two d orbitals may take on the role of the e″ ring orbitals (see **13**). The structure that results is shown in **14**

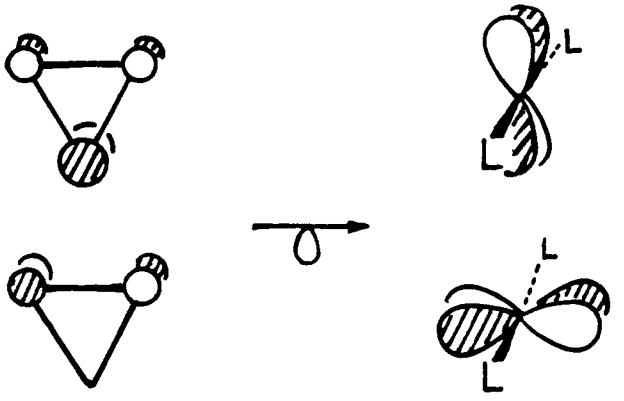

13

and is a layer structure held together by linkages which form a honeycomb array.[13] If this structure were adopted by a compound in which the transition metal has a d^1 configuration the results might prove very interesting. In Figure 5 the π DOS is plotted for the case where X = P, M = Mo, L = H. Such a compound would be nearly ideal because the relatively long Mo–P distance (taken here to be 2.3 Å) mandates a very weak through-space Mo–Mo interaction (Mo–Mo = 3.98 Å). Figure 5 shows an obvious resemblance to Figure 1, only here the superdegenerate band arises from Mo d orbitals. What would be the nature of the electronic ground state? Before addressing this question we must first consider the possibilities for localization of superdegenerate band states.

(9) (a) Sigwarth, B.; Zsolnai, L.; Berke, H.; Huttner, G. *J. Organomet. Chem.* **1982**, *226*, C5. (b) Huttner, G.; Weber, U.; Sigwarth, B.; Scheidsteger, O. *Angew. Chem.* **1982**, *94*, 210; *Angew. Chem., Int. Ed. Engl.* **1982**, *21*, 215. (c) Huttner, G.; Sigwarth, B.; Scheidsteger, O.; Zsolnai, L.; Orama, O. *Organometallics* **1985**, *4*, 326.

(10) Mewis, A. *Z. Naturforsch., Teil B* **1984**, *39*, 713.

(11) Actually, a band which is symmetric with respect to reflection in the plane of the layer overlaps with the nonbonding antisymmetric π^* band and makes a definitive assignment of the valence band impossible. Of course, this does not alter the point being made here.

(12) Hoffmann, R. *Angew. Chem.* **1982**, *21*, 711, and references therein.

(13) Such layers are imbedded in *covellite* CuS; see: na) Alsēn, N. *Geol. Foeren. Stockholm Foerh.* **1931**, *53*, 111. (b) Oftedal, I. *Z. Kristallogr. Mineral.* **1932**, *A83*, 9. (c) Hulliger, F. *Struct. Bonding (Berlin)* **1968**, *4*, 83. (d) Pearson, W. B. "The Crystal Chemistry and Physics of Metals and Alloys"; Wiley: New York, 1972.

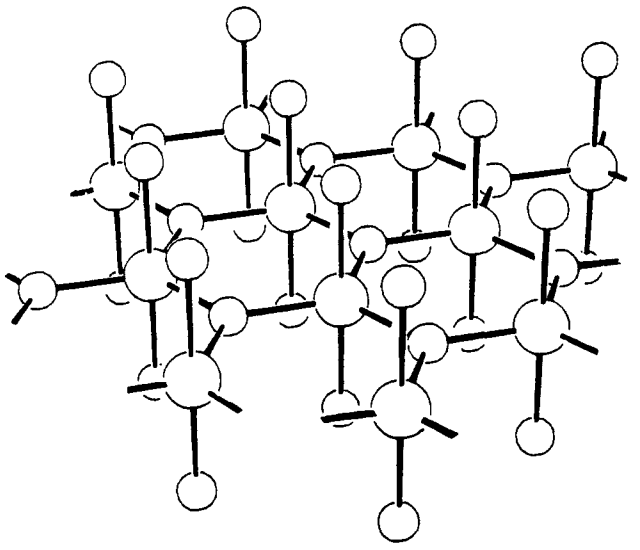

14

Localization

When narrow bands result from the weak interaction between orbitals of the constituent molecules of a crystal, it is correct to assume that the crystal orbitals associated with these bands are little different from their molecular parents. An orthonormal set of functions known as Wannier functions[14] (defined as in eq 10) are very useful in discussing the transition from delocalized to localized states. They can be made optimally localized by a suitable choice of phases for the crystal orbitals for the band in question.

$$\omega_n(\mathbf{R}) = \frac{1}{N^{1/2}}\sum_{\mathbf{k}}^{BZ} e^{-i\mathbf{k}\cdot\mathbf{R}}\psi_n(\mathbf{k}) \quad (n = \text{band index}) \qquad (10)$$

When $\psi_n(\mathbf{k})$ is overwhelmingly dominated by the contribution made by a single molecular orbital ($\psi_n(\mathbf{k}) \sim \sum_{\mathbf{R}} e^{i\mathbf{k}\cdot\mathbf{R}}\eta(\mathbf{r}-\mathbf{R})$), then the form of the Wannier functions approximately reduces to that of the molecular orbitals ($\omega_n(\mathbf{R}) \sim \eta(\mathbf{r}-\mathbf{R})$). In the case of the superdegenerate bands discussed above, it is not possible to construct such localized Wannier functions even though superdegenerate bands are flat (perfectly so, in the simple Hückel model). We will discuss this feature utilizing the ReO_3 case as an illustration of the general points to be made.

The simplest way to understand the nature of the Wannier functions for the superdegenerate oxide p band in ReO_3 is to recognize that they are constrained to be orthogonal to the Re d_{xy} orbitals. It can be seen by inspection that the combination of p orbitals illustrated in **15a** is the most localized such combination which is indeed orthogonal to the d_{xy} orbitals on the four

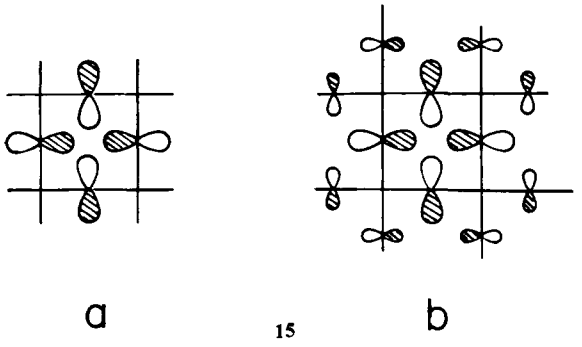

15

(14) (a) Wannier, G. H. *Phys. Rev.* **1937**, *52*, 191. For a review giving many results on Wannier functions, see: (b) Blount, E. I. "Solid State Physics, Advances in Research and Applications"; Seltz, F., Turnbull, D., Ehrenreich, H., Eds.; Academic Press: New York, 1962; Vol. 13, 305. Also see: (c) des Clolzeaux, J. *Phys. Rev. A* **1964**, *135*, 685, 698. (d) Monkhorst, H. J.; Kertesz, M. *Phys. Rev. B: Condens. Matter* **1981**, *24*, 3015.

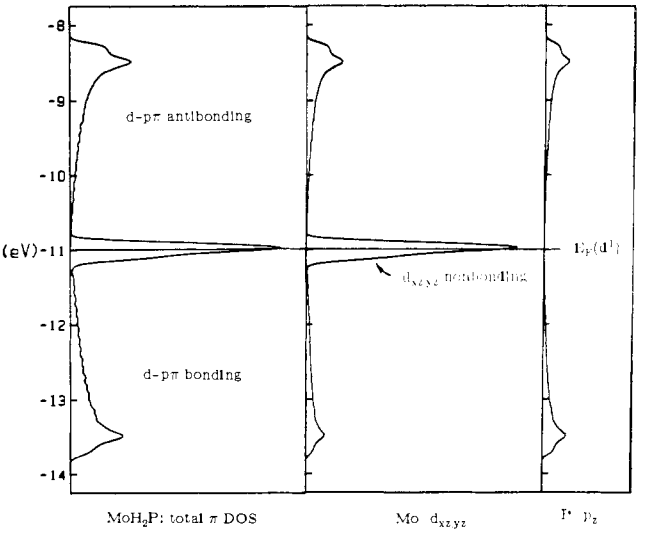

Figure 5. At left the total π DOS for a MoH_2P layer is shown. In the center and right panels respectively the Mo $\{d_{xz},d_{yz}\}$ and P p_z contributions are shown. Note that the Fermi level for a d^1 system is situated in the middle of the superdegenerate d band.

metal centers included in the illustration. However, a set of functions such as **15a** centered at *each lattice site* are not mutually orthogonal; functions centered on neighboring sites have an overlap equal to 1/4. Since the Wannier functions are an orthonormal set, orthogonalization of these functions must be carried out to obtain their correct (and maximally localized) form.[15] This orthogonalization is straightforward if somewhat tedious, the obvious result being an even further delocalization of the Wannier functions beyond four centers, as shown in **15b**.

The delocalized Wannier functions discussed above should be contrasted with the more usual situation that obtains for narrow band systems. Consider, for example, the simplest of extended systems, a chain of H atoms. If the interatomic spacing is sufficiently wide, then we certainly expect the electrons to localize; that is, an electron will prefer to remain on a given center rather than experience the electron repulsion which will result if it shares a site with another electron. Put another way, if the range of energy between the most bonding and antibonding orbitals is small (as it will be when interatomic overlap is small), electron repulsion will cause the electrons to localize. This behavior is reflected in the nature of the Wannier functions for such a system. If interatomic overlap is small, then neighboring s orbitals can be "mutually orthogonalized" by adding a small contribution to each orbital from the neighboring sites, as illustrated in **16**a. When

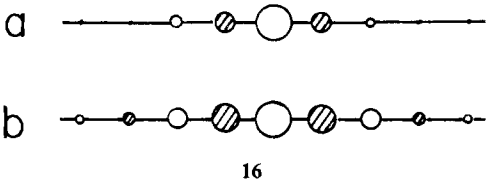

16

the atoms are brought close together, the interatomic overlap grows as does the width of the s band. The electrons will now be more appropriately described as occupying delocalized orbitals starting with those which are most bonding. The poorer localization of the Wannier functions reflects this change; the tails of these functions must grow longer to ensure their mutual orthogonalization (see **16b**). This is in contrast to the characteristics we have described for narrow superdegenerate bands; while these bands are quite narrow, the Wannier functions remain as delocalized as in the wide band case.

The above results call into question the often made implicit assumption that Wannier functions associated with narrow bands

(15) Further localization is possible if one abandons the requirement of orthogonalization; see: (a) Anderson, P. W. *Phys. Rev. Lett.* **1968**, *21*, 13. (b) Anderson, P. W. *Phys. Rep.* **1984**, *110*, 311.

are necessarily highly localized.[16] One area in which this may have an important physical effect is in the formation of excitons by the promotion of an electron from a valence band in a semiconductor to the conduction band. If the valence (or conduction) band is superdegenerate then the hole (or electron) in the excitonic state may be considerably more delocalized than would have been expected solely on the basis of the *width* of the superdegenerate band involved. Further localization of the hole (or electron) is possible by mixing contributions in from bands not formally involved in the excitation, but this will be limited by the cost of raising the "orbital energy" contribution to any excitons formed. For example, in perovskites such as $BaTiO_3$ or $KNbO_3$ (related to ReO_3 as discussed above), excitations from the valence (superdegenerate) O p levels may include the formation of excitons, but the localization of the hole will not be as great as might be expected from the narrow width of the valence band.

The nature of systems in which superdegenerate levels are partially occupied should be more interesting. Insight into these cases is gained by drawing on analogies to molecular diradicals[17] in which two electrons occupy doubly degenerate (usually nonbonding) molecular orbitals. For example, let us contrast the behavior of cyclobutadiene (CB) and trimethylenemethane (TMM). Energy level schemes for the π electrons *in the planar species* are presented in **17**. The relative energies of the states

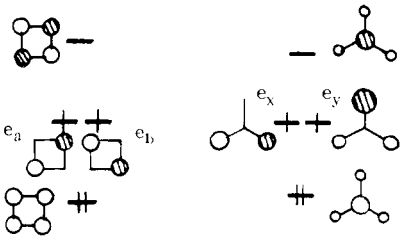

17

derived from the ground configurations for both of these species have been the subject of intense experimental and theoretical scrutiny. However, it is instructive to examine the simple state diagrams shown in **18**. In CB one expects both the $^3A_{2g}$ *and* the

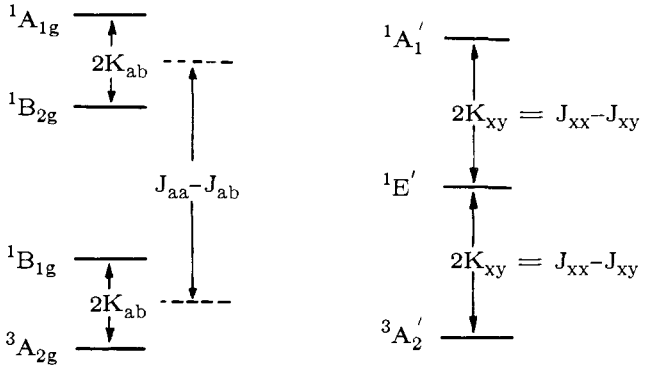

18

$^1B_{1g}$ states to lie low in energy, separated only by a small exchange splitting: $2K_{ab}$. In TMM, however, the $^3A_2'$ state is expected to lie well below the lowest singlet, $^1E'$, by a large exchange energy: $2K_{xy}$. As pointed out by Borden and Davidson,[18] the difference in these two splittings is due to the fact that in CB the degenerate e_g orbitals can be completely localized on different centers (as illustrated) while in TMM the e'' orbitals *must* spread over common centers. The triplet wave functions for both molecules are such that the electrons avoid occupying the same AO's at the same time (by the Pauli principle). Only for CB where the e_a and e_b functions spread over different atoms can a singlet state ($^1B_{1g}$) also avoid on-site repulsions.[19]

The systems we have discussed are clearly like TMM: a localized set of orbitals derived from superdegenerate band orbitals have large intersite overlap densities. We can predict that a half-filled superdegenerate band should lead to a ferromagnetic (i.e., high-spin) ground electronic state[20] in order to avoid the large electron–electron repulsion which will occur when the Wannier functions have large intersite overlap densities. Fundamentally, this is just an extension of ideas put forward for molecules and rests on a simple criterion concerning the localizability of the Hückel MO's for the system under consideration.

Table I. Parameters for EH Calculations

	orb.	H_{ii} (eV)	ζ_1 (c_1)[a]	ζ_2 (c_2)[a]
P	3s	−18.6	1.88	
	3p	−12.5	1.63	
As	4s	−16.22	2.23	
	4p	−12.16	1.89	
Mo	5s	−8.77	1.96	
	5p	−5.60	1.90	
	4d	−11.06	4.54 (0.5899)	1.90 (0.5899)
Pt	6s	−9.08	2.55	
	6p	−5.47	2.55	
	5d	−12.59	6.01 (0.6334)	2.696 (0.5513)

[a] Exponents: double-ζ d functions are used for transition metals.

Acknowledgment. Thanks are due to the Dow Chemical Co. for their support of this research. I owe special thanks to Professor J. K. Burdett for his support and encouragement and for helpful discussions. Thanks are also due to Stephen Lee for first bringing the superdegeneracy found in the 9–3 net to my attention and stimulating this work.

Appendix I

Some of the analytical details of the ReO_3 problem will now be presented. We take up the discussion which was cut short following eq 8 in the text. The orthonormal combination of $p_x(\mathbf{k})$ and $p_y(\mathbf{k})$, to be called $\phi(\mathbf{k})$, will interact with $d_{xy}(\mathbf{k})$, and a 2 × 2 secular equation can be set up involving these functions. For $\chi(\mathbf{k})$ and $\phi(\mathbf{k})$, we obtain:

$$\chi(\mathbf{k}) = \frac{1}{\sqrt{4 - 2\cos(k_x a) - 2\cos(k_y a)}}[(1 - e^{-ik_x a})p_x(\mathbf{k}) - (1 - e^{-ik_y a})p_y(\mathbf{k})] \quad \text{(A1)}$$

$$\phi(\mathbf{k}) = \frac{1}{\sqrt{4 - 2\cos(k_x a) - 2\cos(k_y a)}}[(1 - e^{ik_y a})p_x(\mathbf{k}) + (1 - e^{ik_x a})p_y(\mathbf{k})] \quad \text{(A2)}$$

and the secular equation involving $d_{xy}(\mathbf{k})$ and $\phi(\mathbf{k})$ is

$$\begin{vmatrix} \epsilon_d - \epsilon(\mathbf{k}) & \beta_{dp}(\mathbf{k}) \\ \beta_{dp}^*(\mathbf{k}) & \epsilon_p - \epsilon(\mathbf{k}) \end{vmatrix} = 0 \quad \text{(A3)}$$

where ϵ_d and ϵ_p are respectively the Re(d) and O(p) orbital energies. The wavevector $\mathbf{k}$ ranges over the Brillouin zone, and in all of these equations it is sufficient to restrict one's attention to the region of $\mathbf{k}$-space in which $-\pi/a \leq k_x, k_y \leq \pi/a$. The magnitude of $\beta_{dp}(\mathbf{k})$ is related to the Hückel dπ–pπ resonance integral β_{dp} by the relation:

(16) (a) Whangbo, M.-H. *J. Chem. Phys.* **1980**, *73*, 3854. (b) Brandow, B. H. *Adv. Phys.* **1977**, *26*, 651, and references therein.

(17) (a) For a review of theoretical and experimental aspects of diradicals, see: "Diradicals"; Borden, W. T., Ed.; Wiley: New York, 1982. (b) Salem, L. "Electrons in Chemical Reactions: First Principles"; Wiley: New York, 1982; Chapter 3.

(18) Borden, W. T.; Davidson, E. R. *J. Am. Chem. Soc.* **1977**, *99*, 4587.

(19) Some of the electron repulsion of the $^1E'$ state is relieved by "symmetry breaking" when configuration interaction included in the description of wave function; see ref 17a.

(20) Actually, this is only what is expected for the "zero-temperature" ground state. Whether a system will display ferromagnetism at finite temperatures depends on its dimensionality; e.g., see: Landau, L. D.; Lifshitz, E. M. "Statistical Physics"; Pergamon: Oxford, 1958.

$$|\beta_{dp}(\mathbf{k})|^2 = 2\beta_{dp}{}^2[2 - \cos(k_x a) - \cos(k_y a)] \quad (A4)$$

The solution to the secular equation is:

$$\epsilon(\mathbf{k}) = \langle\epsilon_{dp}\rangle \pm \sqrt{(\Delta\epsilon_{dp}/2)^2 + |\beta_{dp}(\mathbf{k})|^2} \quad (A5)$$

where $\langle\epsilon_{dp}\rangle = (\epsilon_d + \epsilon_p)/2$ and $\Delta\epsilon_{dp} = |\epsilon_d - \epsilon_p|$. Eliminating $\langle\epsilon_{dp}\rangle$ by choice of the energy zero, an exact solution for the density of states, $g(\epsilon)$, can be obtained from the formula for the band dispersion in eq A5:

$$g(\epsilon) = \frac{4|\epsilon|}{\pi^2\beta_{dp}{}^2}K([E^2(2 - E^2)]^{1/2}] \quad (A6a)$$

$K(z)$ is a complete elliptic integral of the first kind;[21] E is restricted to the range $0 \le E^2 \le 2$ and is related to ϵ by the equation:

$$E^2 = \frac{\epsilon^2 - (\Delta\epsilon_{dp}/2)^2}{4\beta_{dp}{}^2} \quad (A6b)$$

The π DOS has the form shown in Figure 2 where $\Delta\epsilon_{dp} = 1.0$ eV, and $|\beta_{dp}| = 1.8$ eV.

The form of the Wannier functions for the superdegenerate band can be determined from eq 10 and A1:

$$\omega(0) = \frac{1}{N^{1/2}}\sum_{\mathbf{k}}^{BZ}\chi(\mathbf{k}) = N^{1/2}(a/2\pi)^2\int_{-\pi/a}^{\pi/a}\int\chi(\mathbf{k})\,dk_x\,dk_y \quad (A7)$$

where the Wannier function considered is that centered on the origin ($\mathbf{R} = 0$). After simplification, expressions for the Wannier function coefficients can be derived. The magnitude of the "inner" orbital coefficients illustrated in **15b** was determined by numerical integration:

$$\frac{4}{\pi^2}\int_{2^{-1/2}}^{1}\frac{E(x) - x_1{}^2K(x)}{x_1x^2\sqrt{2x^2 - 1}}\,dx \approx 0.47239 \quad (A8)$$

$K(x)$ and $E(x)$ are complete elliptic integrals of the first and second kind, respectively, and $x_1 \equiv (1 - x^2)^{1/2}$. This value indicates that 89.3% of the electron density resides on the "inner" centers, which is to be compared to 100% implied by **15a**. The remainder of the electron density resides on centers further removed.

Appendix II

All the computations were carried out using a program employing the extended Hückel method[22a] which may be used for both molecular and crystal calculations. It has been developed to its present state by M.-H. Whangbo, S. Wijeyesekera, M. Kertesz, C. N. Wilker, C. Zheng, and the author. The weighted Wolfsberg–Helmholz formula[22b,c] was used for the H_{ij} matrix elements. Pt and As parameters were taken from ref 6; Mo parameters are from ref 23. Exponents for P and As are originally from ref 24; the P p orbital energy was extrapolated from Herman–Skillman[25] tables so that is in alignment with EH parameters of adjacent elements of the periodic table. Exponents for the transition metals are originally from ref 26. See Table I.

In the results reported for $^2_\infty[Pt_3(As_2)_2{}^{2-}]$ and $^2_\infty[MoH_2P]$ layers in Figures 4 and 5, matrix elements were computed between atoms separated by less than 6.55 Å. Both are two dimensional hexagonal systems in which $^1/_{12}$th of the Brillouin zone was covered by **k**-point meshes: 105 points were used for $^2_\infty[Pt_3(As_2)_2{}^{2-}]$; 300 points were used for $^2_\infty[MoH_2P]$.

(21) (a) Whittaker, E. T.; Watson, G. N. "Modern Analysis", 4th ed.; Cambridge University Press: Cambridge, 1927. (b) Gradshteyn, I. S.; Ryzhik, I. M. "Tables of Integrals, Series, and Products", 4th ed.; Academic Press: New York, 1965.

(22) (a) Hoffmann, R. *J. Chem. Phys.* **1963**, *39*, 1397. (b) Ammeter, J. H.; Bürgi, H.-B.; Thibeault, J. C.; Hoffmann, R. *J. Am. Chem. Soc.* **1978**, *100*, 3686. (c) Summerville, R. H.; Hoffmann, R. *Ibid.* **1976**, *98*, 7240.
(23) Kubâcek, P.; Hoffmann, R.; Havlas, Z. *Organometallics* **1982**, *1*, 180.
(24) Clementi, E.; Roetti, C. *At. Nucl. Data Tables* **1974**, *14*, 177.
(25) Herman, F.; Skillman, S. "Atomic Structure Calculations"; Prentice Hall: Englewood Cliffs, N.J., 1963.
(26) Baranovskii, V. I.; Nikolskii, A. B. *Teor. Eksp. Khim.* **1967**, *3*, 527.

Gas-Phase Isotope Fractionation Factor for Proton-Bound Dimers of Methoxide Anions

David A. Weil[†] and David A. Dixon*[‡]

Contribution from the Department of Chemistry, University of California—Riverside, Riverside, California 92521, and E. I. du Pont de Nemours & Co., Central Research and Development Department, Experimental Station, Wilmington, Delaware 19898. *Received June 8, 1984*

Abstract: The gas-phase isotope fractionation factor, ϕ_{gp}, for A_2L^- (where A = MeO and L = H or D) has been measured by ion cyclotron resonance spectroscopy. The value for ϕ_{gp} is 0.33 ± 0.06. The gas-phase value is compared with the solution measurements. Ab initio calculations on the electronic structure of the dimer have been performed at the DZ+P level. The dimer is found to be asymmetric with a central barrier to proton transfer on the order of 2 kcal/mol. The harmonic force field for the dimer has been determined with the 4-31G basis set. These results are used to calculate a theoretical value for ϕ_{gp} of 0.37 in excellent agreement with the experimental value. The calculated hydrogen bond strength is 25.6 kcal/mol.

Over the past 15 years, determinations of proton transfer equilibrium constants have increased the understanding of gas-phase reaction dynamics and the effect that solvent molecules have on analogous solution-phase equilibrium.[1] In contrast, the rates of proton transfer reactions are not as easily determined in either the gas or solution phase, especially when the proton donor–acceptor separation is small.[2] A description of the potential energy surface for small proton–acceptor separation would aid in the

[†] University of California—Riverside.
[‡] E. I. du Pont de Nemours & Co. Contribution No. 3755.

(1) (a) D. H. Aue and M. T. Bowers In "Gas Phase Ion Chemistry", M. T. Bowers, Ed., Academic Press, New York, 1979, Vol. 2, C9. (b) R. W. Taft In "Proton-Transfer Reactions", E. Caldin and V. Gold, Eds., Wiley, New York, 1975, p 31. (c) E. M. Arnett, Ibid., p 79. (d) E. M. Arnett, *Acc. Chem. Res.*, **6**, 404 (1973). (e) R. W. Taft In "Progress in Physical Organic Chemistry", R. W. Taft, Ed., Vol. 14, p 247, 1983, Wiley-Interscience, New York.

0002-7863/85/1507-6859$01.50/0